



ISSN: 0067-2904
GIF: 0.851

Preparation and Characterization of Nickel Oxide Thin Films by Electrostatic Spray Technique

Raied K. Jamal*, Qahtan G. Al-Zaidi, Nada Mohamed Saeed, Iman N. Taaban

Department of Physics, College of Science, University of Baghdad, Baghdad, Iraq

Abstract

A simple, inexpensive, and home-built electrostatic spray deposition (ESD) system with stable cone-jet mode was used to obtain nickel oxide (NiO) thin films on glass substrates kept at temperature of 400°C. The primary precursor solution of 0.1 M concentration hydrated nickel chloride dissolved in isopropyl alcohol. The structural, optical and electrical parameters were studied. The optical absorbance spectra for the studied samples showed its maximum around 280 nm. On the other hand, thickness interferometry measurements on the tested samples showed that film thickness was around 400 nm. The optical energy gap of the prepared NiO samples was determined to be 3.75 eV and the maximum value of refractive index was determined to be 2.1 at 350 nm.

Keywords: Electrostatic spray deposition; Nickel oxide; Thin films; Optical properties

تحضير ودراسة خصائص الاغشية الرقيقة لأكسيد النيكل المحضرة بتقانه الرش الكهربائي المستقر

رائد كامل جمال*، قحطان كاطع الزيدي، ندى محمد سعيد، ايمان ناجي تعبان

قسم الفيزياء، كلية العلوم، جامعة بغداد، بغداد، العراق

الخلاصة

تم استخدام طريقة ترسيب الرش الكهربائي المستقر البسيطة وغير المكلفة والمتجانسة للحصول على اغشية رقيقة لأكسيد النيكل المرسبة على قواعد زجاجية بدرجة حرارية 400 سيليزي. المحلول الاولي كان كلورايد النيكل المهدرج المذاب في ايسوبروبيل الكحول بتركيز 0.1 مولاري. ثم دراسة الخصائص التركيبية والكهربائية والبصرية ولذلك طيف الامتصاص البصري للاغشية المحضرة اظهرت اعلى قيمة لها عند الطول الموجي 280 نانو متر. وكذلك، تم قياس السمك بطريقة التداخل البصري حيث ان سمك الاغشية كان حوالي 400 نانومتر. فجوة الطاقة البصرية للاغشية والعينات المحضرة حددت ب 3.75 إلكترون فولت واقصى قيمة لمعامل الانكسار كان بحدود 2.1 عند 350 نانومتر.

1. Introduction

As a transition metal oxide, nickel oxide (NiO) is described as an NaCl-like antiferromagnetic semiconductor. It is a promising candidate for many recent applications such as solar thermal absorber [1], catalyst for O₂ evolution [2], photoelectrolysis [3] and electrochromic device [4] and positive electrode in batteries [5], while the pure stoichiometric NiO crystals are perfect insulators [6]. Various methods and techniques, such as vacuum evaporation [7], electron beam evaporation [8], RF-magnetron sputtering [9], anodic oxidation [10], chemical deposition [11], atomic layer epitaxy [12], sol-gel [13] and spray pyrolysis technique (SPT) [14], were employed to prepare NiO thin films.

In this work, NiO thin films have deposited from aqueous solution of nickel chloride on glass substrates by ESD technique and studied their structures, optical properties, surface morphology and roughness.

*Email: raiedkamel@yahoo.com

2. Experiment

Chemical techniques for thin film preparation are intensively studied as they facilitate the designing of materials at molecular level. Amongst, ESD results in good productivity from a simple apparatus. The setup of ESD system is schematically illustrated in Figure-1 [15]. It is essentially made up of a precursor solution, electrostatic HV-DC power supply, precursor atomization nozzle assembly, and a temperature-controlled hot-plate heater. The atomizer has an adjustable steel capillary tube of 0.25 mm inner diameter nozzle clamped to a holder and supported by a metal tripod. The prepared precursor solution to be sprayed is flowing through the nozzle due to gravity with a flow rate ranging from 0.2 to 1 ml/min. A simple high frequency (14–42 kHz) and variable duty-cycle circuit is built for the DC high voltage power supply used in measurements. The NE 555 timer drives the flyback transformer in the “Flyback mode”. Due to the high voltage applied at the metal needle, a Taylor cone-jet is created at the tip of the nozzle and the solution disrupts upon the droplets charge density reach rayleigh limit after which the spray starts [16].

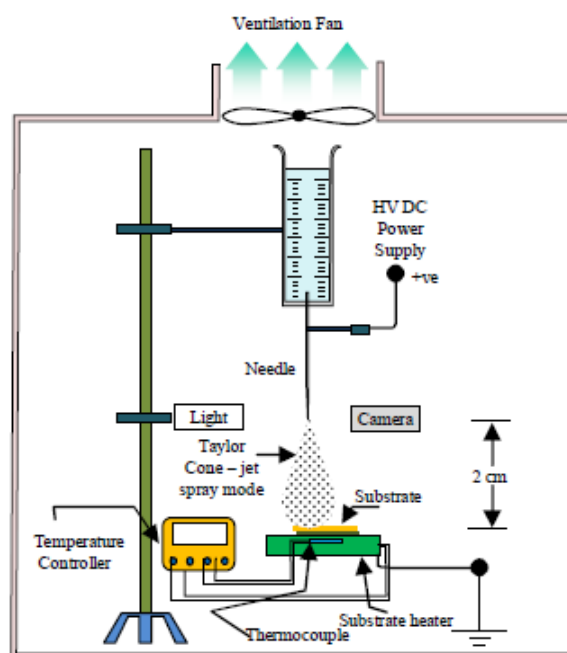


Figure 1- Electrostatic Spray Deposition (ESD) experimental set up [16].

A 0.1 M concentration aqueous precursor solution of $\text{NiCl}_2 \cdot 6\text{H}_2\text{O}$ (molecular weight of 237.7048 g/mole) has been prepared by dissolving a solute quantity of 1.2 g of $\text{NiCl}_2 \cdot 6\text{H}_2\text{O}$ in 100 ml isopropyl alcohol ($\text{C}_3\text{H}_8\text{O}$). A magnetic stirrer is used for this purpose for 10-15 minutes together with addition of 0.1 ml HCl acid to facilitate the complete dissolution of the solute in the solvent ($\text{C}_3\text{H}_8\text{O}$). Prior to deposition of the films, the commercial glass substrates were thoroughly cleaned in distilled water and dried in air for 5 min. After that, they were soaked in ethanol to remove any stains and contaminants. The electrostatic spray is conducted at substrate temperature within 400°C during the deposition. Film thickness is controlled by both the precursor concentration and the number of sprays, or alternatively, spraying time. Thus, a 4-second spray time is maintained during the experiment. The normalized distance between the spray nozzle and substrate was fixed at 2 cm. The spray rate of solution was maintained at 0.2 ml/min throughout the experiment. Nickel chloride solution was sprayed onto the preheated glass substrate, so, it evaporates, the solute precipitates and pyrolytic decomposes, resulting in the formation of NiO films according to the following reaction:



The as-prepared films were gray in color, uniform and strongly adherent to the substrate.

3. Result and Discussion

The XRD patterns of films deposited at 400°C showed amorphous and polycrystalline structures before and after annealing, respectively, at 450°C for three hours as presented in Fig. (2). The XRD peaks indicate a cubic phase structure for NiO thin films as the intensity of the (100), (111) and (200) peaks increases with increasing annealing temperature. Table (1) gives the essential XRD data, which

include the FWHM and the (hkl) of the main diffraction peaks. Also, the grain size is evaluated using the well-known Scherrer's formula [17] as:

$$G = \frac{0.94\lambda}{\beta \cos\theta} \quad (2)$$

Where G is the average crystalline grain size, λ is the x-ray wavelength (1.5406 Å), β is the full-width at half maximum (FWHM) of the peak (in radians) and θ is the Bragg's diffraction angle of the XRD peak (in degrees). The calculated values of grain size for NiO thin film were found to vary between 21.5–20 nm at different planes. While Figure-3 shows an SEM image, in which the grains of the sprayed NiO thin film are observed.

The optical characteristics involving the optical energy gap (E_g) and the optical constants (i.e., refractive index n, extinction coefficient k, real dielectric constant ϵ_r and imaginary dielectric ϵ_i) of the prepared NiO films were studied within the range 280-780 nm. The absorbance spectrum shown in Figure-4 shows a high band gap semiconductor with absorption edge in the UV region and no absorption edge in the visible region. The obtained data were analyzed to calculate the band gap energy of the NiO films using classical relation. Figure-5 shows the variation of $(\alpha h\nu)^2$ as a function of incident photon energy ($h\nu$) for NiO thin films. It can be observed from this figure that the energy gap is equal to 3.75 eV as estimated from the extrapolation of the linear part of the spectrum to $(\alpha h\nu)^2$ value of zero, Tauc relation [18]. Our results are in good agreement to the reported values of energy band gap of NiO ranging in 3.4-3.8 eV.. The variation of NiO film refractive index with wavelength is shown in Figure-6, as it is almost constant within the range 380-1000 nm and decreases with decreasing wavelength. Figure-7 shows the variation of extinction coefficient with wavelength and it is observed that the extinction coefficient is slightly changed in the visible region. Also, it is observed that the extinction coefficient is increasing highly with increasing wavelength shorter than 360nm oppositely to the variation of the refractive index, but the minimum values are observed at 360 nm. Figures-8, and -9 show the variation of real (ϵ_r) and imaginary (ϵ_i) dielectric constants of the prepared NiO thin films. One can observe that the variation of (ϵ_r) has a similar trend to that of the refractive index because of the smaller values of k^2 in comparison with n^2 , while the variation of (ϵ_i) mainly depends on the k value, which is related to the variation of absorption coefficient and represents the absorption of radiation by free carriers. It is also observed that the real and imaginary dielectric constants increase with increasing wavelength of the incident radiation in the range 300-360 nm and this behavior is due to the change of reflectance and absorbance, while they are constant in the region longer than 360 nm.

Figure-10 shows the photoluminescence response of one of prepared NiO samples. The characteristics were examined by exciting the sample using an incident light of 3.06 eV energy at 405 nm wavelength. Emission characteristics showed two peaks, the first is around 405 nm and the other is around 450 nm.

4. Conclusion

NiO thin films were deposited by spraying solution on to the glass substrates using a simple and inexpensive ESD technique at 400°C. The XRD studies show that the film deposited was NiO (cubic phase) with orientation along (111) direction. The optical absorption measurements showed that the NiO films had flat surfaces, high average absorbance around 280 nm, and direct band gap energy of 3.75 eV.

Table 1-Diffraction data for the NiO electrostatically-sprayed samples

Peak No.	2 θ (deg)	(hkl)	G (Å)
1	33	100	20
2	37	111	20.2
3	44	200	20.2
4	64	220	21.5

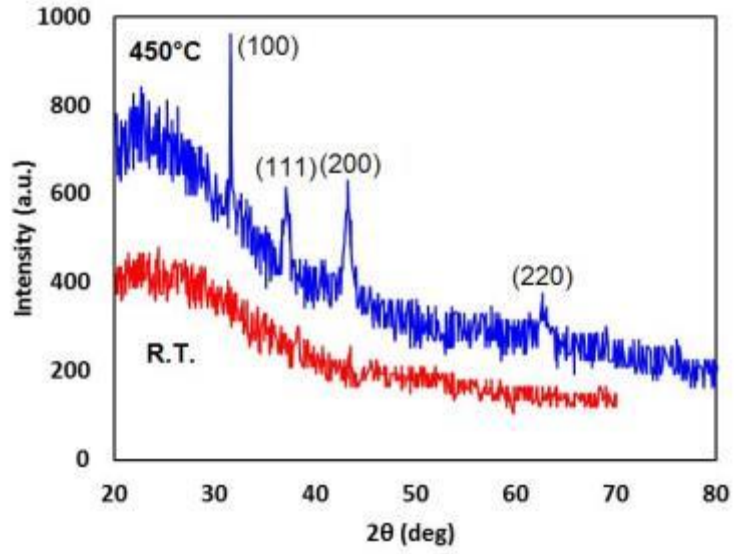


Figure 2-XRD pattern of NiO thin film (a) before annealing and (b) after annealing at 450°C.

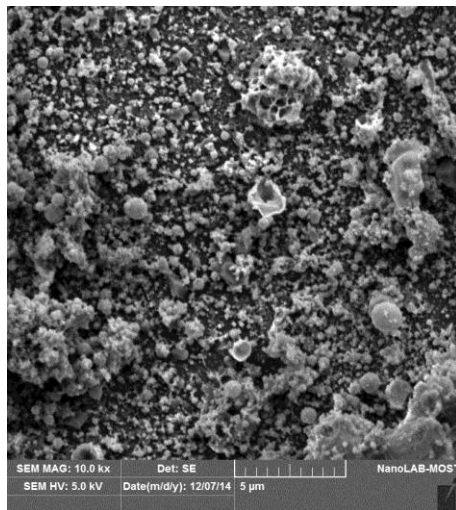


Figure 3-SEM image showing sub- micrometer grain size of the sprayed NiO thin film before annealing.

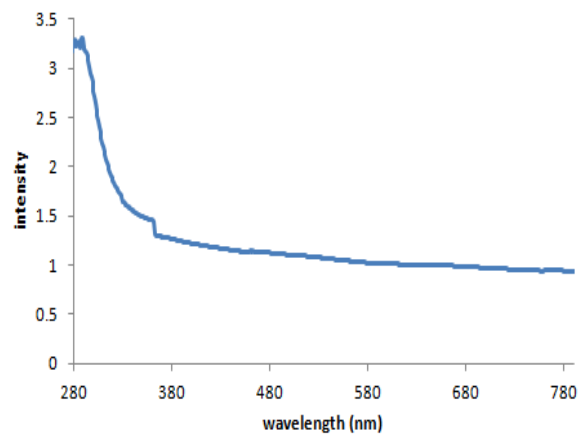


Figure 4-The optical absorbance of NiO thin films.

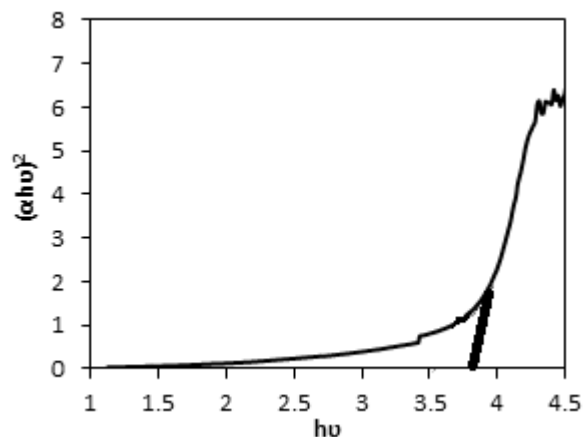


Figure 5 -Variation of $(\alpha h\nu)^2$ versus $h\nu$ eV for NiO thin films.

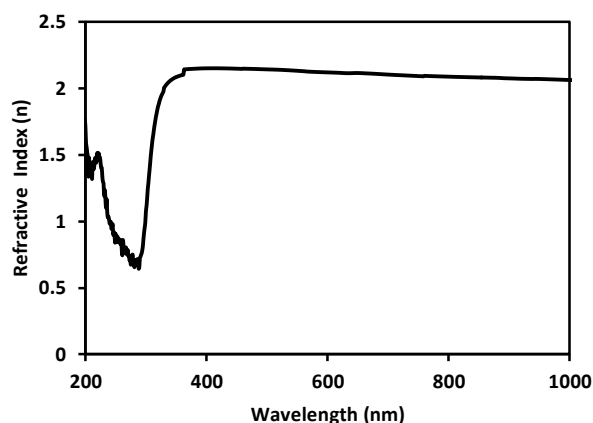


Figure 6-The refractive index (n) for NiO thin films at room temperature

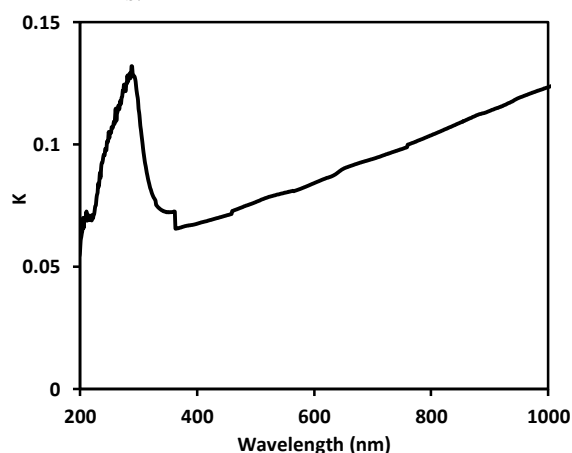


Figure 7-The extinction coefficient for NiO thin films at room temperature.

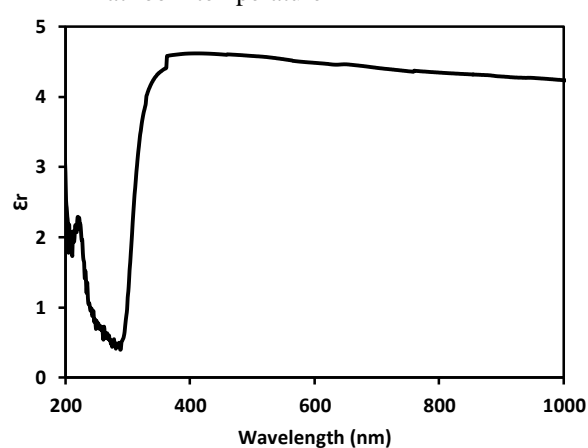


Figure 8- Real dielectric constant ϵ_r for NiO thin films

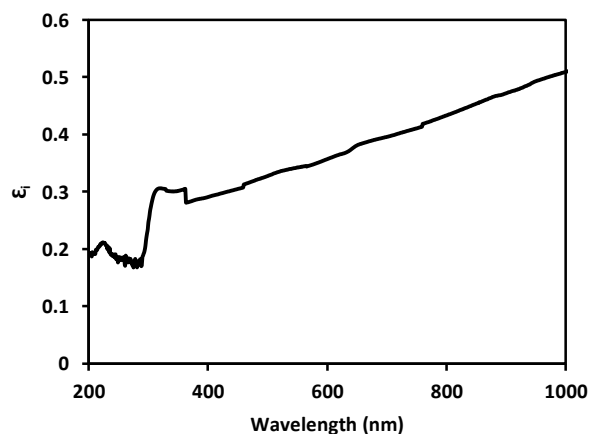


Figure 9- Imaginary dielectric constant ϵ_i for NiO thin films

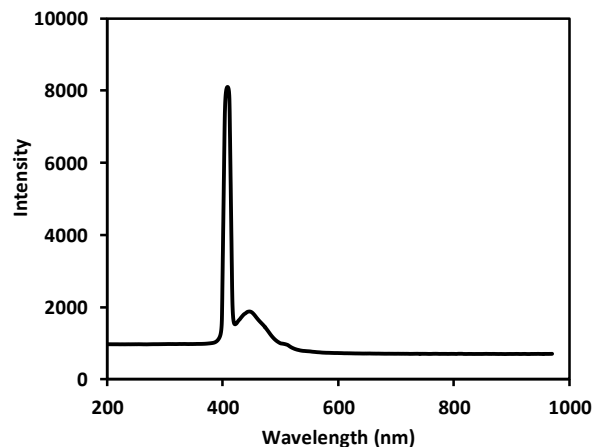


Figure 10-The fluorescence spectra for NiO thin films

References

1. Cook, J.G. and Koffyberg, F.P. **1984**. Solar thermal absorbers employing oxides of Ni and Co. *Solar Energy Mater.* 10(1), pp:55-67.
2. Botejue, J.C.N. and Tseung, A.C.C. **1985**. Oxygen Evolution on Nickel Oxide Electrodes. *J. Electrochem. Soc.* 132(12), pp: 2957-2959.
3. Koffyberg, F.P. and Benko, F.A. **1981**. p-Type NiO as a Photoelectrolysis Cathode. *J. Electrochem. Soc.* 128(11), pp: 2476-2479.
4. Lampert, C.M. **1984**. Electrochromic materials and devices for energy efficient windows. *Solar Energy Mater.* 11, pp:1-27.

5. C.A. Vincent, F. Bonion, M. Lizzari and B. Scrosati. **1987**. *Modern Batteries*. First Edition. Edward Arnold. London.
6. Bosman, A.J. and Crevecoeur, C. **1966**. Mechanism of the Electrical Conduction in Li-Doped NiO. *Phys. Rev.* 144(2), p:763.
7. Tsu, R., Esaki, L. and Ludeke, R. **1969**. IBM Research Note RC-2418.
8. Seike, T. and Nagai, J. **1991**. *Solar Energy Mater.* 22, p:107.
9. Sato, H., Minami, T., Takato, S. and Yamada, T. **1993**. Transparent conducting p-type NiO thin films prepared by magnetron sputtering. *Thin Solid Films, Elsevier*, 236(1-2), pp:27-31.
10. Lampert, C.M., Omstead, T.R. and Tu, P.C. **1986**. Spectroscopic and Electrochemical Studies of Electrochromic Hydrated Nickel Oxide Films. *Solar Energy Materials*, 16, pp:1-17.
11. Varkey, A.J. and Fort, A.F. **1993**. Solution growth technique for deposition of nickel oxide thin films. *Thin Solid Films, Elsevier*, 235(1-2), pp:47-50.
12. Chigane, M., Ishikawa, M. and Chem, J. **1993**. Metal Oxide Scale Interfacial Imperfections and Performance of Stainless Steels Utilized as Interconnects in Solid Oxide Fuel Cells, *Journal of The Electrochemical Society*, 156, pp:765-770.
13. Utriainen, M., Kroger-Laukkanen, M. and Niinisto, L. **1998**. Studies of NiO thin film formation by atomic layer epitaxy. *Materials Science and Engineering: B* 54, pp: 98-103.
14. Surca, A., Orel, B., Pilhar, B. and Bwkovec, P. **1996**. Chemical vapor deposition at low temperature. *J. Electroanal. Chem.* 408. p:83.
15. Al-Ansari, M.S., Al-Zaidi, Q.G. and Hasan, S.I. **2014**. Hydrogen Sensing Characteristics of Electrostatically Sprayed Palladium – Doped Tin Dioxides. *Int. J. Application or Innovation in Eng. Manage. IJAIEM*. 3(3). March.
16. Wilm, M.S. and Mann, M. **1994**. Elec-trostatic deposition of nanothin films on metal substrate. *Int. J. Mass Spectro. Ion Proc.*, 136, pp:167-180.
17. Kumar, S.S., Venkateswarlu, P., Rao, V.R. and Rao, G.N. **2013**. The NO₂ sensing ITO thin films prepared by ultrasonic spray pyrolysis. *Inter. Nano Lett.*, pp:3-30.
18. Mehta, S.K., Kumar, S., Chaudhary, S. and Bhasin, K.K. **2009**. Effect of surfactant head groups on synthesis, growth and agglomeration behavior of ZnS nanoparticles. *Nanoscale Res.Lett.* 4, pp: 1197-1208.